ISSN 1063-7761, Journal of Experimental and Theoretical Physics, 2012, Vol. 114, No. 4, pp. 547–554. © Pleiades Publishing, Inc., 2012.
Original Russian Text © S.V. Blazhevich, I.V. Kolosova, A.V. Noskov, 2012, published in Zhurnal Eksperimental'noi i Teoreticheskoi Fiziki, 2012, Vol. 141, No. 4, pp. 627–635.

ATOMS, MOLECULES, OPTICS

Coherent X-ray Radiation Generated by a Relativistic Electron in an Artificial Periodic Structure

S. V. Blazhevich[a], I. V. Kolosova[b], and A. V. Noskov[b]

[a] *Belgorod State University, Belgorod, 308015 Russia*

[b] *Belgorod University of Consumer Cooperatives, Belgorod, 308023 Russia*

e-mail: noskovbupk@mail.ru

Received January 26, 2011

Abstract—A theory of coherent X-ray radiation from a relativistic electron crossing an artificial periodic layered structure in the Laue scattering geometry is constructed. The expressions describing the spectral-angular radiation parameters are obtained. It is shown that the radiation yield in such a medium may substantially exceed the radiation yield in a crystal under analogous conditions.

DOI: 10.1134/S1063776112020021

1. INTRODUCTION

The emission of radiation from a relativistic particle in a periodic layered structure has been traditionally considered in the Bragg scattering geometry for the case when reflecting layers are parallel to the input surface (i.e., for the case of symmetric reflection). Radiation in a periodic layered structure was usually considered as resonant transition radiation [1, 2]. In [3], radiation from a multilayer periodic structure was represented as the sum of diffracted transition radiation (DTR) and parametric X-ray radiation (PXR). In the above publications, radiation from a relativistic particle in a multilayer medium was considered in the Bragg scattering geometry for the particular case of symmetric reflection of the particle field relative to the target surface (for diffracting layers parallel to the target surface). In [3], radiation was analyzed analogously to coherent radiation induced by a relativistic electron in a crystalline medium [4–7].

Here, we develop a dynamic theory of coherent radiation in an artificial periodic structure in the Laue scattering geometry for an arbitrary asymmetry of reflection of the electron field relative to the target surface (i.e., for an arbitrary angle between the reflecting structure and the target surface). An important feature of the geometry considered here is that in contrast to the traditional Bragg scattering geometry [1–3], emitted photons move forward and intersect the target. The possibility of changing the photon yield of coherent radiation in a crystal due to dynamic effects in radiation (in particular, asymmetry in the field reflection relative to the target surface) has been demonstrated earlier [8–10]. The influence of the reflection asymmetry on the radiation yield in a crystal is confirmed by the results of experiments in [11]. In [10], coherent X-ray radiation in a direction close to that of the velocity of a relativistic electron crossing the crystal was considered as the sum of the contributions of forward parametric X-ray radiation (FPXRs) and transition radiation (TR) (Fig. 1).

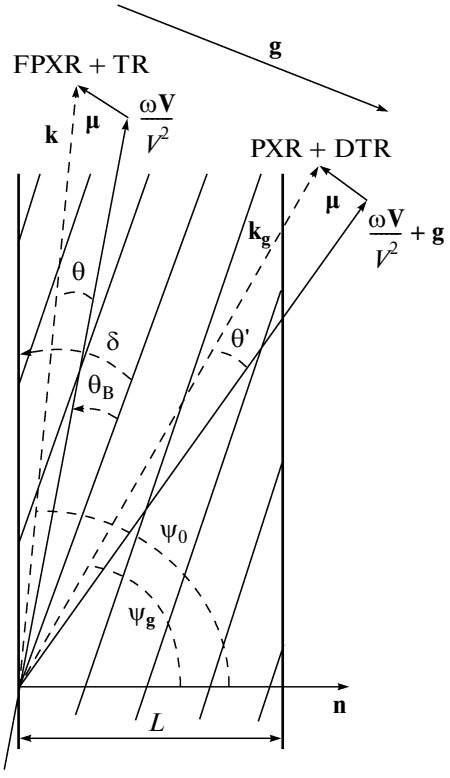

Fig. 1. Geometry of emission: θ and θ' are angles of incidence of radiation, θ_B is the Bragg angle, δ is the angle between the plate surface and the diffracting layers, and **k** and $\mathbf{k_g}$ are the wavevectors of the incident and diffracted photons.

In this paper, we consider coherent radiation generated by a relativistic electron in an artificial periodic medium as a result of operation of two coherent radiation mechanisms (PXR and DTR). Emission occurs in a different direction (see Fig. 1), namely, in the direction of Bragg scattering of pseudophotons of the Coulomb field of an electron from a system of diffracting layers of the target material. The expressions for the spectral-angular radiation density induced by a relativistic electron crossing the artificial multilayer periodic structure formed by alternating layers of substances with sharply differing permittivities in the considered radiation frequency range will be obtained using the two-wave approximation of the dynamic diffraction theory. Analysis of these expressions shows that dynamic diffraction effects can noticeably manifest themselves in the radiation emitted by a relativistic electron in a periodic layered medium. Moreover, it is shown that under almost analogous conditions, the photon yield in a periodic layered structure is almost an order of magnitude higher than the photon yield in a crystalline medium due to the dynamic effects.

2. RADIATION FIELD AMPLITUDE

Suppose that a relativistic electron crosses at velocity $\mathbf{V}$ a multilayer structure (see Fig. 1) of thickness L, which is formed by periodically arranged amorphous layers with thicknesses a and b ($T = a + b$ is the period of the structure) and susceptibilities χ_a and χ_b, respectively. In Fig. 1, $\boldsymbol{\mu} = \mathbf{k} - \omega\mathbf{V}/V^2$ is the momentum component of a virtual photon, which is perpendicular to velocity $\mathbf{V}$ ($\mu = \omega\theta/V$, where $\theta \ll 1$ is the angle between vectors $\mathbf{k}$ and $\mathbf{V}$), θ_B is the Bragg angle, and φ is the azimuthal angle of incidence of radiation measured from the plane formed by electron velocity vector $\mathbf{V}$ and vector $\mathbf{g}$ perpendicular to the reflecting layers. The length of vector $\mathbf{g}$ can also be expressed in terms of the Bragg angle and Bragg frequency ω_B: $g = 2\omega_B \sin\theta_B/V$.

In [10], a theory of coherent X-rays propagating in the direction of vector $\mathbf{k}$ (see Fig. 1) close to the direction of the velocity of a relativistic electron was constructed, in which radiation was treated as the sum of FPXR and TR. However, in the two-wave approximation of dynamic diffraction theory [12], each photon moving in direction $\mathbf{k}$ corresponds to a photon propagating in direction $\mathbf{k}_\mathbf{g} = \mathbf{k} + \mathbf{g}$ (see Fig. 1), and waves from one direction are permanently pumped in the crystal in the other direction and back. Here, we consider radiation from a relativistic electron in an artificial periodic structure in the $\mathbf{k}_\mathbf{g}$ direction. Having performed analytic procedures for the $\mathbf{k}_\mathbf{g}$ direction, which are analogous to the procedures described in [10], we obtain for radiation in the $\mathbf{k}$ direction the following expressions for the radiation field as the sum of the contributions from the PXR an DTR:

$$E_\mathbf{g}^{(s)\mathrm{Rad}} = E_\mathrm{PXR}^{(s)} + E_\mathrm{DTR}^{(s)}, \tag{1a}$$

$$\begin{aligned}
E_\mathrm{PXR}^{(s)} = {} & -\frac{8\pi^2 ieV\theta P^{(s)}}{\omega}\frac{\omega^2\chi_\mathbf{g}C^{(s)}}{\lambda_0^*} \\
& \times\left[8\frac{\gamma_0}{\gamma_\mathbf{g}}\sqrt{\beta^2 + 4\chi_\mathbf{g}\chi_{-\mathbf{g}}C^{(s)^2}\frac{\gamma_\mathbf{g}}{\gamma_0}}\right]^{-1} \\
& \times\left\{\left(\beta + \sqrt{\beta^2 + 4\chi_\mathbf{g}\chi_{-\mathbf{g}}C^{(s)^2}\frac{\gamma_\mathbf{g}}{\gamma_0}}\right)\right. \\
& \times\left[\left(1 - \exp\left(-i\frac{\lambda_\mathbf{g}^* - \lambda_\mathbf{g}^{(2)}}{\gamma_\mathbf{g}}L\right)\right)(\lambda_\mathbf{g}^* - \lambda_\mathbf{g}^{(2)})^{-1}\right] \\
& -\left(\beta - \sqrt{\beta^2 + 4\chi_\mathbf{g}\chi_{-\mathbf{g}}C^{(s)^2}\frac{\gamma_\mathbf{g}}{\gamma_0}}\right) \\
& \left.\times\left[\left(1 - \exp\left(-i\frac{\lambda_\mathbf{g}^* - \lambda_\mathbf{g}^{(1)}}{\gamma_\mathbf{g}}L\right)\right)(\lambda_\mathbf{g}^* - \lambda_\mathbf{g}^{(1)})^{-1}\right]\right\} \\
& \times\exp\left[i\left(\frac{\omega\chi_0}{2} + \lambda_g^*\right)\frac{L}{\gamma_g}\right],
\end{aligned} \tag{1b}$$

$$\begin{aligned}
E_\mathrm{DTR}^{(s)} = {} & \frac{8\pi^2 ieV\theta P^{(s)}}{\omega}\frac{\chi_\mathbf{g}C^{(s)}}{\frac{\gamma_0}{\gamma_\mathbf{g}}\sqrt{\beta^2 + 4\chi_\mathbf{g}\chi_{-\mathbf{g}}C^{(s)^2}\frac{\gamma_\mathbf{g}}{\gamma_0}}} \\
& \times\left(\frac{\omega}{-\omega\chi_0 - 2\lambda_0^*} + \frac{\omega}{2\lambda_0^*}\right) \\
& \times\left[\exp\left(-i\frac{\lambda_\mathbf{g}^* - \lambda_\mathbf{g}^{(1)}}{\gamma_\mathbf{g}}L\right) - \exp\left(-i\frac{\lambda_\mathbf{g}^* - \lambda_\mathbf{g}^{(2)}}{\gamma_\mathbf{g}}L\right)\right] \\
& \times\exp\left[i\left(\frac{\omega\chi_0}{2} + \lambda_\mathbf{g}^*\right)\frac{L}{\gamma_\mathbf{g}}\right].
\end{aligned} \tag{1c}$$

Expressions (1b) and (1c) are the amplitudes of the PXR and DTR fields, respectively, in the direction of the Bragg vector (vector $\mathbf{k}_\mathbf{g}$ in Fig. 1). It is noteworthy that these expressions differ from those for the corresponding field amplitudes (see expressions (18b) and (18c) in [10]) in the direction of the velocity of an electron emitting FPXR and TR (vector $\mathbf{k}$ in Fig. 1).

In expressions (1), we used the following notation, which is analogous to that from [10]:

$$\begin{aligned}
\lambda_\mathbf{g}^{(1,2)} = {} & \frac{\omega|\chi_\mathbf{g}'|C^{(s)}}{2}\left\{\xi^{(s)} - \frac{i\rho^{(s)}(1-\varepsilon)}{2}\right. \\
& \left.\pm\left[\xi^{(s)^2} + \varepsilon - 2i\rho^{(s)}\left(\frac{1-\varepsilon}{2}\xi^{(s)} + \kappa^{(s)}\varepsilon\right)\right.\right. \\
& \left.\left. - \rho^{(s)^2}\left(\frac{(1-\varepsilon)^2}{4} + \kappa^{(s)^2}\varepsilon\right)\right]^{1/2}\right\},
\end{aligned} \tag{2}$$

$$\lambda_0^* = \omega\left(\frac{\gamma^{-2}+\theta^2-\chi_0}{2}\right), \quad \lambda_{\mathbf{g}}^* = \frac{\omega\beta}{2}+\frac{\gamma_{\mathbf{g}}}{\gamma_0}\lambda_0^*,$$

$\gamma_0 = \cos\psi_0$, $\gamma_{\mathbf{g}} = \cos\psi_{\mathbf{g}}$, ψ_0 being the angle between wavevector $\mathbf{k}$ of the incident wave and vector $\mathbf{n}$ normal to the plate surface and $\psi_{\mathbf{g}}$ being the angle between wavevector $\mathbf{k}_{\mathbf{g}}$ and vector $\mathbf{n}$ (see Fig. 1), and

$$\xi^{(s)}(\omega) = \eta^{(s)}(\omega)+\frac{1-\varepsilon}{2\nu^{(s)}},$$

$$\eta^{(s)}(\omega) = \frac{\sin^2\theta_B}{V^2C^{(s)}}\frac{gT}{|\chi_b'-\chi_a'||\sin(ga/2)|}$$

$$\times\left(1-\frac{\omega(1-\theta\cos\varphi\cot\theta_B)}{\omega_B}\right),$$

$$\nu^{(s)} = \frac{2C^{(s)}|\sin(ga/2)|}{g}\left|\frac{\chi_b'-\chi_a'}{a\chi_a'+b\chi_b'}\right|,$$

$$\rho^{(s)} = \frac{a\chi_a''+b\chi_b''}{|\chi_b'-\chi_a'|C^{(s)}2|\sin(ga/2)|}\frac{g}{}, \tag{3}$$

$$\kappa^{(s)} = \frac{2C^{(s)}|\sin(ga/2)|}{g}\left|\frac{\chi_b''-\chi_a''}{a\chi_a''+b\chi_b''}\right|,$$

$$\varepsilon = \frac{\gamma_{\mathbf{g}}}{\gamma_0}, \quad C^{(1)} = 1, \quad C^{(2)} = \cos2\theta_B,$$

$$P^{(1)} = \sin\varphi, \quad P^{(2)} = \cos\varphi.$$

For the value of parameter $s = 1$, radiation field amplitudes (1) describe σ-polarized fields, while for $s = 2$, these amplitudes describe π-polarized fields.

Quantities χ_0 and $\chi_{\mathbf{g}}$ for the artificial periodic structure under investigation have the form

$$\chi_0(\omega) = \frac{a}{T}\chi_a+\frac{b}{T}\chi_b,$$

$$\chi_{\mathbf{g}}(\omega) = \frac{e^{-iga}-1}{igT}(\chi_b-\chi_a), \tag{4}$$

$$\chi_0' = \frac{a}{T}\chi_a'+\frac{b}{T}\chi_b', \quad \chi_0'' = \frac{a}{T}\chi_a''+\frac{b}{T}\chi_b''.$$

An important parameter in expression (2) is parameter ε, which can be written in the form

$$\varepsilon = \frac{\sin(\delta+\theta_B)}{\sin(\delta-\theta_B)}; \tag{5}$$

this parameter determines the degree of asymmetry of reflection of the fields relative to the target surface. Here, θ_B is the angle between the electron velocity and reflecting layers and δ is the angle between the surface of the target and the reflecting layers. It should be noted that the angle of incidence $\delta-\theta_B$ of an electron on the target surface increases with decreasing parameter ε (Fig. 2). In the symmetric case, the wavevectors of incident and diffracted photons form equal angles with the surface of the plate, while in the case of asymmetric reflection, these angles are different (see Fig. 2). Here, $\varepsilon = 1$ and $\delta = \pi/2$ in the symmetric case and $\varepsilon \neq 1$ and $\delta \neq \pi/2$ in the asymmetric case.

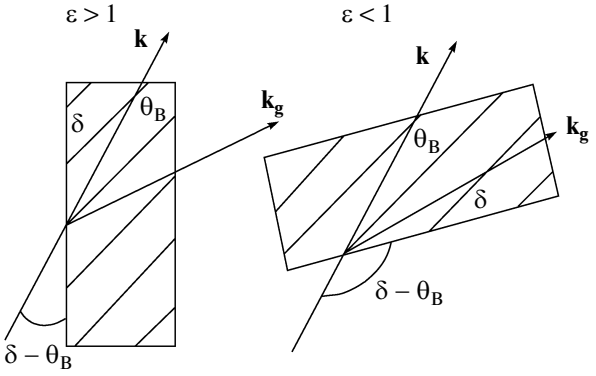

Fig. 2. Asymmetric (ε > 1, ε < 1) reflections of radiation from the target. The case ε = 1 corresponds to symmetric reflection.

Substituting expression (2) into (1b) and (1c), we can write the latter expressions in the form

$$E_{\mathrm{PXR}}^{(s)} = \frac{4\pi^2ieV}{\omega}\frac{\theta P^{(s)}}{\theta^2+\gamma^{-2}-\chi_0}$$

$$\times\left\{\frac{\xi^{(s)}+\sqrt{\xi^{(s)^2}+\varepsilon}}{\sqrt{\xi^{(s)^2}+\varepsilon}}\right.$$

$$\times\left[1-\exp\left(-ib^{(s)}\left(\sigma^{(s)}+\frac{\xi^{(s)}+\sqrt{\xi^{(s)^2}+\varepsilon}}{\varepsilon}\right)\right.\right.$$

$$\left.\left.-b^{(s)}\rho^{(s)}\Delta^{(2)}\right)\right]$$

$$\times\left(\sigma^{(s)}+\frac{\xi^{(s)}+\sqrt{\xi^{(s)^2}+\varepsilon}}{\varepsilon}-i\rho^{(s)}\Delta^{(2)}\right)^{-1}$$

$$-\frac{\xi^{(s)}-\sqrt{\xi^{(s)^2}+\varepsilon}}{\sqrt{\xi^{(s)^2}+\varepsilon}} \tag{6a}$$

$$\times\left[1-\exp\left(-ib^{(s)}\left(\sigma^{(s)}+\frac{\xi^{(s)}-\sqrt{\xi^{(s)^2}+\varepsilon}}{\varepsilon}\right)\right.\right.$$

$$\left.\left.-b^{(s)}\rho^{(s)}\Delta^{(1)}\right)\right]$$

$$\left.\times\left(\sigma^{(s)}+\frac{\xi^{(s)}-\sqrt{\xi^{(s)^2}+\varepsilon}}{\varepsilon}-i\rho^{(s)}\Delta^{(1)}\right)^{-1}\right\}$$

$$\times \exp\left[i\left(\frac{\omega\chi_0}{2}+\lambda_{\mathbf{g}}^*\right)\frac{L}{\gamma_{\mathbf{g}}}\right],$$

$$E_{\mathrm{DTR}}^{(s)} = \frac{4\pi^2 ieV}{\omega}\theta P^{(s)}\left(\frac{1}{\theta^2+\gamma^{-2}}\right.$$

$$\left.-\frac{1}{\theta^2+\gamma^{-2}-\chi_0}\right)\frac{\varepsilon}{\sqrt{\xi^{(s)^2}+\varepsilon}}$$

$$\times\left\{\exp\left[-ib^{(s)}\left(\sigma^{(s)}+\frac{\xi^{(s)}-\sqrt{\xi^{(s)^2}+\varepsilon}}{\varepsilon}\right)\right.\right.$$

$$\left.-b^{(s)}\rho^{(s)}\Delta^{(1)}\right] \qquad (6b)$$

$$-\exp\left[-ib^{(s)}\left(\sigma^{(s)}+\frac{\xi^{(s)}+\sqrt{\xi^{(s)^2}+\varepsilon}}{\varepsilon}\right)\right.$$

$$\left.\left.-b^{(s)}\rho^{(s)}\Delta^{(2)}\right]\right\}$$

$$\times \exp\left[i\left(\frac{\omega\chi_0}{2}+\lambda_{\mathbf{g}}^*\right)\frac{L}{\gamma_{\mathbf{g}}}\right],$$

where

$$\Delta^{(2)} = \frac{\varepsilon+1}{2\varepsilon}+\frac{1-\varepsilon}{2\varepsilon}\frac{\xi^{(s)}}{\sqrt{\xi^{(s)^2}+\varepsilon}}$$

$$+\frac{\kappa^{(s)}}{\sqrt{\xi^{(s)^2}+\varepsilon}},$$

$$\Delta^{(1)} = \frac{\varepsilon+1}{2\varepsilon}-\frac{1-\varepsilon}{2\varepsilon}\frac{\xi^{(s)}}{\sqrt{\xi^{(s)^2}+\varepsilon}}$$

$$-\frac{\kappa^{(s)}}{\sqrt{\xi^{(s)^2}+\varepsilon}}, \qquad (7)$$

$$\sigma^{(s)} = \frac{1}{|\chi_{\mathbf{g}}'|C^{(s)}}(\theta^2+\gamma^{-2}-\chi_0')$$

$$\equiv \frac{1}{\nu^{(s)}}\left(\frac{\theta^2}{|\chi_0'|}+\frac{1}{\gamma^2|\chi_0'|}+1\right),$$

$$b^{(s)} = \frac{\omega\left|\mathrm{Re}\sqrt{\chi_{\mathbf{g}}\chi_{-\mathbf{g}}}\right|C^{(s)}}{2}\frac{L}{\gamma_0}.$$

The PXR yield is mainly formed by only one of the branches corresponding to the second term in expression (6a). This can easily be verified directly, but the real part of the denominator in this term vanishes. The solution to the corresponding equation

$$\sigma^{(s)}+\frac{\xi^{(s)}-\sqrt{\xi^{(s)^2}+\varepsilon}}{\varepsilon} = 0 \qquad (8)$$

defines frequency ω_* in the whose vicinity the spectrum of PXR photons emitted at a fixed angle of observation is concentrated.

Substituting expressions (6a), (6b), and (1a) into the well-known [13] expression for the spectral-angular density of X-rays,

$$\omega\frac{d^2N}{d\omega d\Omega} = \omega^2(2\pi)^{-6}\sum_{s=1}^{2}\left|E_{\mathbf{g}}^{(s)\mathrm{Rad}}\right|^2, \qquad (9)$$

we obtain the following expressions describing the contributions from the PXR and DTR mechanisms to the spectral-angular density of radiation, including that for the term that results from the interference of these radiation mechanisms (subscript "INT"):

$$\omega\frac{d^2N_{\mathrm{PXR}}^{(s)}}{d\omega d\Omega}$$

$$= \frac{e^2}{4\pi^2}P^{(s)^2}\frac{\theta^2}{\left(\theta^2+\gamma^{-2}-\chi_0'\right)^2}R_{\mathrm{PXR}}^{(s)}, \qquad (10a)$$

$$R_{\mathrm{PXR}}^{(s)} = \left(1-\frac{\xi}{\sqrt{\xi^2+\varepsilon}}\right)^2$$

$$\times\left\{1+\exp(-2b^{(s)}\rho^{(s)}\Delta^{(1)})\right.$$

$$-2\exp(-b^{(s)}\rho^{(s)}\Delta^{(1)}) \qquad (10b)$$

$$\left.\times\cos\left[b^{(s)}\left(\sigma^{(s)}+\frac{\xi-\sqrt{\xi^2+\varepsilon}}{\varepsilon}\right)\right]\right\}$$

$$\times\left[\left(\sigma^{(s)}+\frac{\xi-\sqrt{\xi^2+\varepsilon}}{\varepsilon}\right)^2+\rho^{(s)^2}\Delta^{(1)^2}\right]^{-1},$$

$$\omega\frac{d^2N_{\mathrm{DTR}}^{(s)}}{d\omega d\Omega} = \frac{e^2}{4\pi^2}P^{(s)^2}\theta^2$$

$$\times\left(\frac{1}{\theta^2+\gamma^{-2}}-\frac{1}{\theta^2+\gamma^{-2}-\chi_0'}\right)^2R_{\mathrm{DTR}}^{(s)}, \qquad (11a)$$

$$R_{\mathrm{DTR}}^{(s)} = \frac{4\varepsilon^2}{\xi^2+\varepsilon}\exp\left(-b^{(s)}\rho^{(s)}\frac{1+\varepsilon}{\varepsilon}\right)$$

$$\times\left[\sin^2\left(b^{(s)}\frac{\sqrt{\xi^2+\varepsilon}}{\varepsilon}\right)\right. \qquad (11b)$$

$$\left.+\sinh^2\left(b^{(s)}\rho^{(s)}\frac{(1-\varepsilon)\xi^{(s)}+2\varepsilon\kappa^{(s)}}{2\xi\sqrt{\xi^2+\varepsilon}}\right)\right],$$

$$\omega\frac{d^2N_{\rm INT}^{(s)}}{d\omega d\Omega}=\frac{e^2}{4\pi^2}P^{(s)^2}\theta^2\left(\frac{1}{\theta^2+\gamma^{-2}}-\frac{1}{\theta^2+\gamma^{-2}-\chi_0'}\right)\frac{1}{\theta^2+\gamma^{-2}-\chi_0'}R_{\rm INT}^{(s)},\tag{12a}$$

$$\begin{aligned}R_{\rm INT}^{(s)}=&-\frac{2\varepsilon}{\xi^{(s)^2}+\varepsilon}{\rm Re}\left\{\left(\xi^{(s)}-\sqrt{\xi^{(s)^2}+\varepsilon}\right)\right.\\&\times\left[1-\exp\left(-ib^{(s)}\left(\sigma^{(s)}+\frac{\xi^{(s)}-\sqrt{\xi^{(s)^2}+\varepsilon}}{\varepsilon}\right)\right.\right.\\&\left.\left.-b^{(s)}\rho^{(s)}\Delta^{(1)}\right)\right]\\&\times\left(\sigma^{(s)}+\frac{\xi^{(s)}-\sqrt{\xi^{(s)^2}+\varepsilon}}{\varepsilon}-i\rho^{(s)}\Delta^{(1)}\right)^{-1}\\&\times\left[\exp\left(ib^{(s)}\left(\sigma^{(s)}+\frac{\xi^{(s)}-\sqrt{\xi^{(s)^2}+\varepsilon}}{\varepsilon}\right)\right.\right.\\&\left.-b^{(s)}\rho^{(s)}\Delta^{(1)}\right)\\&-\exp\left(ib^{(s)}\left(\sigma^{(s)}+\frac{\xi^{(s)}+\sqrt{\xi^{(s)^2}+\varepsilon}}{\varepsilon}\right)\right.\\&\left.\left.\left.-b^{(s)}\rho^{(s)}\Delta^{(2)}\right)\right]\right\}.\end{aligned}\tag{12b}$$

Subsequently integrating expressions (10)–(12) with respect to frequency, we obtain the following expressions describing the angular density of radiation:

$$\frac{dN_{\rm PXR}^{(s)}}{d\Omega}=\frac{e^2P^{(s)^2}\nu^{(s)}}{8\pi^2\sin^2\theta_{\rm B}|\chi_0'|}\times\left(\frac{\theta^2}{|\chi_0'|}+\frac{1}{\gamma^2|\chi_0'|}+1\right)^{-2}\int\limits_{-\infty}^{\infty}R_{\rm PXR}^{(s)}d\eta^{(s)}(\omega),\tag{13}$$

$$\frac{dN_{\rm DTR}^{(s)}}{d\Omega}=\frac{e^2P^{(s)^2}\nu^{(s)}}{8\pi^2\sin^2\theta_{\rm B}|\chi_0'|}\times\left(\frac{\theta^2}{|\chi_0'|}+\frac{1}{\gamma^2|\chi_0'|}+1\right)^{-2}\int\limits_{-\infty}^{\infty}R_{\rm DTR}^{(s)}d\eta^{(s)}(\omega),\tag{14}$$

$$\frac{dN_{\rm INT}^{(s)}}{d\Omega}=\frac{e^2P^{(s)^2}\nu^{(s)}}{8\pi^2\sin^2\theta_{\rm B}|\chi_0'|}\frac{\theta^2}{|\chi_0'|}\left(\frac{\theta^2}{|\chi_0'|}+\frac{1}{\gamma^2|\chi_0'|}+1\right)^{-2}\times\left(\frac{\theta^2}{|\chi_0'|}+\frac{1}{\gamma^2|\chi_0'|}\right)^{-1}\int\limits_{-\infty}^{\infty}R_{\rm INT}^{(s)}d\eta^{(s)}(\omega).\tag{15}$$

The consequent expressions (10)–(12) and (13)–(15) are the main result of this study. Their relations make it possible to analyze the spectral-angular radiation characteristics in an artificial multilayer periodic structure in the Laue scattering geometry taking into account manifestations of dynamic effects both known in the physics of scattering of free X-rays in a crystal [12] and those predicted by the authors for scattering of pseudophotons of the Coulomb field of a relativistic electron in a crystal [8–10].

3. PARAMETERS OF DYNAMIC X-RAY SCATTERING

As mentioned above, the reflections from a multilayer artificial periodic structure are traditionally analyzed only in the Bragg scattering geometry in the symmetric case, when the layers are parallel to the target surface, although radiation in a crystalline medium is mainly studied in the Laue scattering geometry for the reasons familiar to experimenters. The expressions derived here make it possible to analyze the dependence of the radiation parameters on thicknesses a and b of different amorphous media with corresponding dielectric susceptibilities χ_a and χ_b, as well as on symmetry parameter ε (see expression (5)) for a preset Bragg angle $\theta_{\rm B}$, which determines angle δ between the reflecting layers and the target surface.

Parameter $\nu^{(s)}$ (3) assuming values from the interval $0\le\nu^{(s)}\le1$ defines the degree of reflection of the field from the periodic structure, which is determined by the type of interference (constructive with $\nu^{(s)}\approx1$ or destructive with $\nu^{(s)}\approx0$) of the waves reflected from different planes. If $g=2\pi/T$, this parameter can be written in the form

$$\nu^{(s)}=\frac{2C^{(s)}}{g}\left|\sin\frac{\pi a}{T}\right|\left|\frac{\chi_b'-\chi_a'}{a\chi_a'+b\chi_b'}\right|.\tag{16}$$

Parameter $\nu^{(s)}$ is proportional to the angular densities of radiation (13)–(15); if the real parts of the dielectric susceptibilities of the amorphous media constituting the periodic structure are approximately identical ($\chi_b'\approx\chi_a'$), this parameter (as well as the radiation intensity) is small. Expression (16) also implies that in the limiting case when the thickness of any layer tends to zero ($a\longrightarrow0$ or $b\longrightarrow0$), parameter

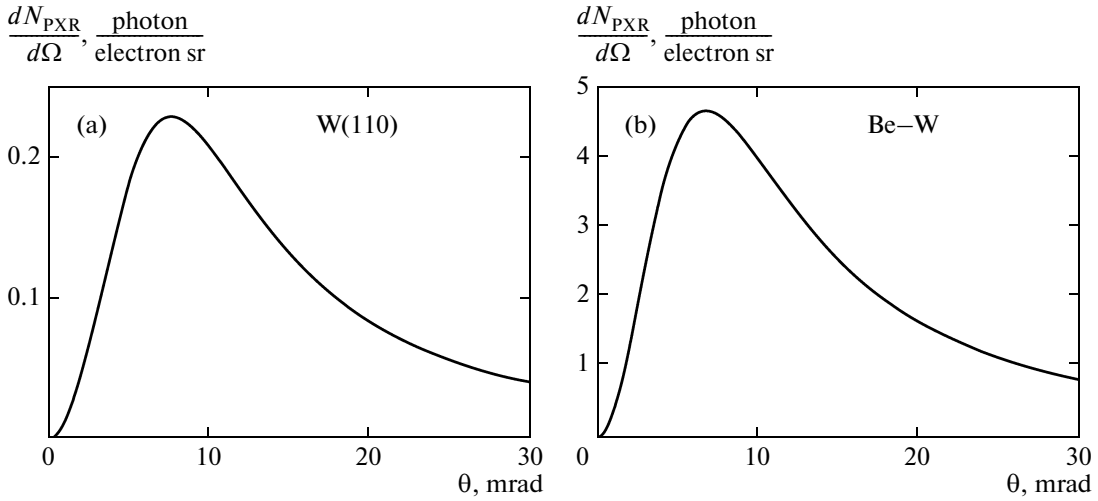

Fig. 3. Angular densities of PXR emitted by a relativistic electron crossing a W crystal plate (a) and Be–W artificial periodic layered structure (b) for $\varepsilon = 3$, $L_e = 56$ μm, $E = 250$ MeV, $\omega_B = 8$ keV, $L = 16$ μm (a), 2 μm (b), $\theta_B = 20°$ (a), 2.2° (b), $\delta = 37°$ (a), 4.5° (b), $N_{\mathrm{ph}} = 6 \times 10^{-4}$ (a), 9×10^{-3} (b), and $a_{\mathrm{Be}} = b_{\mathrm{W}} = 10^{-3}$ μm.

$\nu^{(s)} \longrightarrow 0$, and the medium becomes homogeneous; in this case, there are naturally no reflections because the periodic structure does not exist, $dN/d\Omega = 0$.

Parameter $\rho^{(s)} = L_{\mathrm{ext}}^{(s)}/L_{\mathrm{abs}}$ (3) characterizes the extent of X-ray absorption by a periodic medium and is defined as the ratio of the extinction length

$$L_{\mathrm{ext}}^{(s)} = \frac{gT}{2C^{(s)}\omega}\left|\sin\frac{ga}{2}\right|^{-1}\left|\chi_b' - \chi_a'\right|^{-1}$$

to the absorption length

$$L_{\mathrm{abs}} = \frac{T}{\omega\left|a\chi_a'' + b\chi_b''\right|}$$

for X-rays in the periodic structure. It should be noted that at a depth equal to the extinction length, the energy of the primary wave is pumped completely to the secondary wave propagating in the Bragg direction.

Parameter $\kappa^{(s)}$ (3) defines the extent to which the effect of anomalously low photoabsorption (Borman effect) is manifested in the transmission of X-ray photons through an artificial multilayer periodic structure (this effect is well known in the physics of X-ray scattering in a crystal [14]). The manifestation of the Borman effect in a crystal for coherent X-rays with different symmetries of reflection was studied in [8]. A necessary condition for the manifestation of the Borman effect is $\kappa^{(s)} \approx 1$ both for the crystalline and for the artificial periodic structure. In this case, the expression for $\Delta^{(1)}$ in relations (7) indicates that the value of $\Delta^{(1)}$ decreases upon an increase in parameter $\kappa^{(s)}$; at the same time, the PXR damping decreases (see expression (10b)) because the product $\rho^{(s)}\Delta^{(1)}$ characterizing absorption decreases. Hence it follows that under certain conditions, the Borman effect can also be manifested in the emission of coherent X-rays by a relativistic particle in artificial multilayer periodic structures.

4. NUMERICAL CALCULATIONS

Expressions (10a), (11a), (12a), and (13)–(15) derived above for coherent X-rays emitted by a relativistic charged particle in a periodic multilayer medium formed the basis for numerically calculating the spectral-angular radiation distribution for various parameter values of the diffracting structure (material and thickness of the target layers), the degree of asymmetry in radiation reflection, and the energy of the emitting particle.

To compare the radiation yields from a relativistic particle in a crystal and in an artificial multilayer structure, we plotted the PXR angular density curves ($\omega_B = 8$ keV) for a tungsten (W) crystalline target (Fig. 3a) and for a multilayer periodic structure consisting of amorphous beryllium (Be) layers and W (Fig. 3b). The curves are plotted in accordance with formula (13). The electron path length $L_e = 56$ μm in the target and asymmetry parameter $\varepsilon = 3$ are chosen identical for both cases. It follows from Fig. 3 that the PXR angular density for the multilayer periodic structure exceeds by many times the angular density of PXR from the crystal. The ratio of the total yields of PXR photons is $N_{ph}^{\mathrm{Be–W}}/N_{ph}^{\mathrm{W}} \approx 15$. The increase in the radiation yield is due to the fact that the spectral width for the multilayer periodic structure (Fig. 4b) turns out to be much larger than the spectral width for the crystal (Fig. 4a) because an electron intersects a much smaller number of inho-

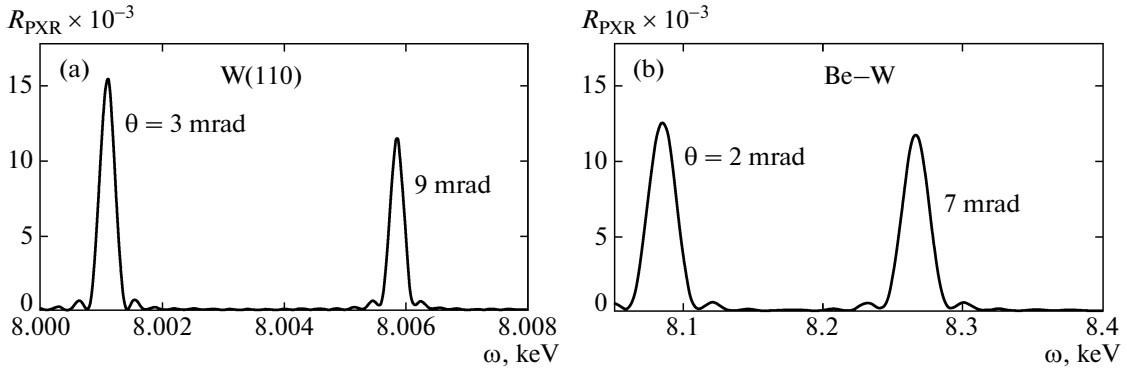

Fig. 4. PXR spectra in the crystalline medium (a) and in Be–W artificial periodic layered structure (b).

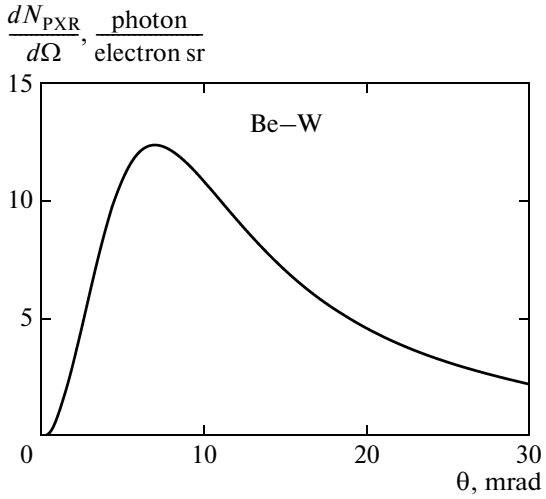

Fig. 5. The same as in Fig. 3b, but for asymmetry parameter $\varepsilon = 6$, $L = 1$ μm, $\delta = 3°$, and $N_{ph} = 2.8 \times 10^{-2}$.

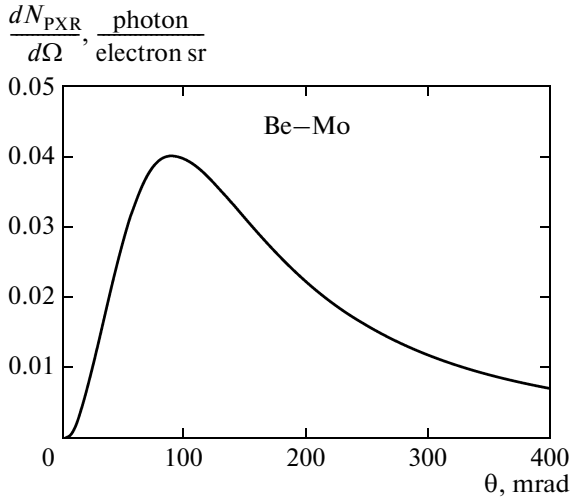

Fig. 6. Angular density of PXR emitted by a relativistic electron crossing a Be–Mo artificial periodic layer structure for $\varepsilon = 11$, $L = 2$ μm, $L_e = 43$ μm, $E = 100$ MeV, $a_{Be} = b_{Mo} = 5 \times 10^{-3}$ μm, $\theta_B = 14°$, $\delta = 17°$, and $N_{ph} = 2 \times 10^{-2}$.

mogeneities in the former case. The curves describing the PXR spectrum and shown in Fig. 4 were plotted using formula (10b).

The radiation yield of emitted photons can also be increased by changing the asymmetry of the field reflection relative to the target surface so that parameter ε becomes larger (Fig. 5). In this case, the PXR spectral density in the multilayer medium and in the crystal [8] increases due to the increase in the peak width in the PXR spectrum, which is associated with a change in the resonance width (8) upon a change in reflection asymmetry parameter ε.

Figures 6–8 show the angular distributions of the angular density of radiation ($\omega_B = 250$ eV) in the case when a relativistic electrons crosses the artificial multilayer periodic structure consisting of beryllium (Be) and molybdenum (Mo) layers. Figure 6 demonstrates a substantial yield of X-rays with an energy of 250 eV (which cannot be attained when a crystal radiator is used); such radiation is widely used, for example, in modern X-ray diagnostics in medicine. The thickness of the multilayer structure (43 μm) for which the curves in Fig. 6 are plotted is high enough to ensure complete absorption of transition radiation generated at the front surface of the structure. The curves for the angular densities of DTR and PXR in Fig. 7 are plotted for the same conditions as in Fig. 6, but for a thin target (4.3 μm) in which DTR is almost not absorbed. The PXR angular density distribution curves in Figs. 6 and 7 have almost the same amplitude due to saturation of the amplitude of radiation from the thick target. Figure 7 shows that the additional contribution to the photon yield of diffracted transition radiation in this case becomes significant; DTR is concentrated in the range of small observation angles. If the energy of an electron incident on the multilayer target increases, the DTR spectral-angular density becomes substan-

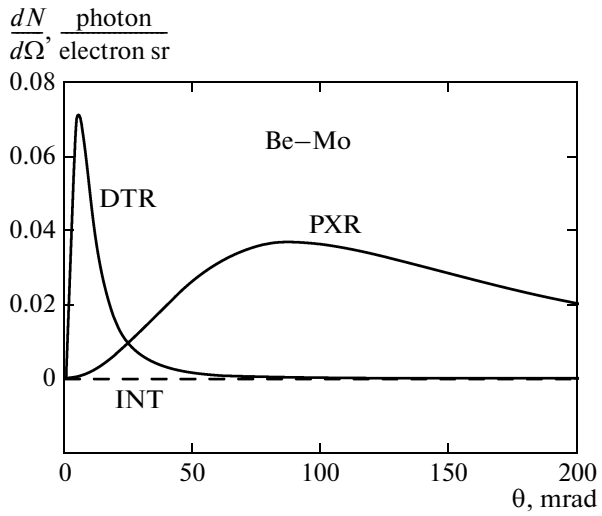

Fig. 7. Angular densities of DTR and PXR. The parameters are the same as in Fig. 6, but the target thickness is different, $L = 0.2$ μm, $L_e = 4.3$ μm.

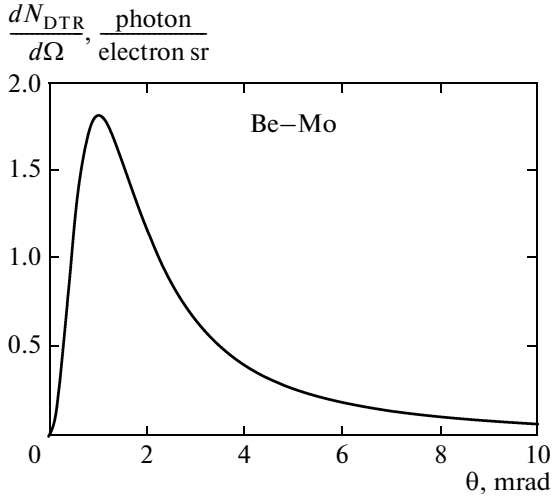

Fig. 8. Angular density of DTR. Parameters are the same as in Fig. 7, but for a higher relativistic electron energy $E =$ 500 MeV.

tially higher, which follows from comparison of the curves in Figs. 7 and 8.

5. CONCLUSIONS

In this study, a theory of coherent X-ray radiation emitted by a relativistic electron crossing an artificial periodic layered structure in the Laue scattering geometry has been developed. The expression describing the spectral-angular characteristics of radiation emitted in the direction of Bragg scattering of pseudophotons of the Coulomb field of the particles are derived. It is shown that the radiation yield in the artificial periodic structure substantially exceeds the radiation yield in a crystal under analogous conditions because the spectral width of radiation from the multilayer periodic structure is larger due to the fact that the number of inhomogeneities crossed by the electron in the target is smaller in this case. The possibility of an additional increase in the photon radiation yield due to a change in asymmetry of reflection is demonstrated. Our results can be used for designing an alternative quasi-monochromatic X-ray source, which can be tuned smoothly in frequency. The high efficiency of an artificial multilayer medium in generating X-rays with an energy on the order of 250 eV, which is widely used in modern X-ray diagnostics in medicine, is demonstrated.

REFERENCES

1. M. L. Ter-Mikaelyan, *High-Energy Electromagnetic Processes in Condensed Media* (Academy of Sciences of the Armenian SSR, Yerevan, 1969; Wiley, New York, 1972).
2. M. A. Piestrup, D. G. Boyers, C. I. Pincus, Q. Li, G. D. Hallewell, M. J. Moran, D. M. Skopik, R. M. Silzer, X. K. Maruyama, D. D. Snyder, and G. B. Rothbart, Phys. Rev. A: At., Mol., Opt. Phys. **45**, 1183 (1992).
3. N. N. Nasonov, V. V. Kaplin, S. R. Uglov, M. A. Piestrup, and C. K. Gary, Phys. Rev. E: Stat., Nonlinear, Soft Matter Phys. **68**, 3604 (2003).
4. G. M. Garibyan and C. Yang, Sov. Phys. JETP **34**, 495 (1971).
5. V. G. Baryshevskii and I. D. Feranchuk, Sov. Phys. JETP **34**, 502 (1971).
6. V. G. Baryshevsky and I. D. Feranchuk, J. Phys. (Paris) **44**, 913 (1983).
7. A. Caticha, Phys. Rev. A: At., Mol., Opt. Phys. **40**, 4322 (1989).
8. S. V. Blazhevich and A. V. Noskov, Nucl. Instrum. Methods Phys. Res., Sect. B **266**, 3770 (2008).
9. S. V. Blazhevich and A. V. Noskov, Nucl. Instrum. Methods Phys. Res., Sect. B **266**, 3777 (2008).
10. S. V. Blazhevich and A. V. Noskov, JETP **109** (6), 901 (2009).
11. Y. Hayakawa, K. Hayakawa, M. Inagaki, T. Kuwada, K. Nakao, K. Nogami, T. Sakai, I. Sato, Y. Takahashi, and T. Tanaka, in *Proceedings of the 51st Workshop of the INFN Eloisatron Project, Erice, Italy, October 25–November 1, 2008* (World Scientific, Singapore, 2010), p. 677.
12. Z. G. Pinsker, *Dynamical Scattering of X-rays in Crystals* (Nauka, Moscow, 1974; Springer, Berlin, 1978).
13. V. A. Bazylev and N. K. Zhevago, *Radiation of High-Energy Particles in the Substances and External Fields* (Nauka, Moscow, 1987) [in Russian].
14. G. Borrmann, Z. Phys. **42**, 157 (1941).

Translated by N. Wadhwa